DOI 10.1007/s11106-017-9898-0
Powder Metallurgy and Metal Ceramics, Vol. 56, Nos. 5-6, September, 2017 (Russian Original Vol. 56, Nos. 5-6, May-June, 2017)

PROTECTIVE AND FUNCTIONAL POWDER COATINGS

HIGH-VELOCITY AIR PLASMA SPRAYING OF (Ti, Cr)C–32 wt.% Ni CLAD POWDER

Yu. S. Borisov,[1,3] A. L. Borisova,[1] M. V. Kolomytsev,[1] O. P. Masyuchok,[1] I. I. Timofeeva,[2] and M. A. Vasilkovskaya[2]

UDC 621.793.7:621.762

The influence of air plasma spraying (parameters such as plasma gun power, spraying distance, plasma gas flow, anode diameter) of (Ti, Cr)C–32 wt.% Ni clad powder on the characteristics of resultant coatings (structure, microhardness, porosity, phase composition) is studied. The experimental procedure is designed using the mathematical planning method. The experimental data are processed to derive regression equations, determining the quantitative dependence of average microhardness and stability of microhardness characteristics on spraying process parameters. It is found that plasma gun power and plasma gas flow have the greatest impact on microhardness of the coatings and $\Delta X/HV^{av}$ parameter, which characterizes the reproducibility of coating properties. The spraying distance has hardly any influence on the properties studied within the test range (160–220 mm). The hardness of coatings produced from the (Ti, Cr)C–32 wt.% Ni clad powder (12.15–14.58 GPa) is higher than that of the coatings obtained by air plasma spraying of a mechanical mixture of 75 wt.% (Ti, Cr)C + 25 wt.% NiCr (5.3–12.6 GPa).

Keywords: *cermets, double titanium–chromium carbide, clad powder, high-velocity air plasma spraying, properties of coatings, microhardness, experimental design.*

INTRODUCTION

Plasma spray coatings of refractory metal carbides have found wide application in wear protection of surfaces at high temperatures and can substantially extend the life of parts for various engineering purposes [1–4]. Possessing high hardness, titanium and chromium carbides are of considerable interest for producing tungsten-free hard alloys [5–11]. Compared to tungsten carbide, titanium and chromium carbides show higher oxidation resistance at 1000°C. In this regard, double titanium–chromium carbide, (Ti, Cr)C, attracts special attention, as it has high microhardness (to 40 GPa), exceeding that of titanium carbide TiC and chromium carbide Cr_3C_2 (32 and 22.8 GPa, respectively) [11]. Double carbide (Ti, Cr)C has also high oxidation resistance in the range 700–1100°C, which is greater than that of TiC (to 900°C) and slightly lower than that of Cr_3C_2 (to 1200°C) [12–16].

[1]Paton Electric Welding Institute, National Academy of Sciences of Ukraine, Kiev, Ukraine. [2]Frantsevich Institute for Problems of Materials Science, National Academy of Sciences of Ukraine, Kiev, Ukraine.

[3]To whom correspondence should be addressed; e-mail: borisov@paton.kiev.ua.

Translated from Poroshkovaya Metallurgiya, Vol. 56, Nos. 5–6 (515), pp. 87–100, 2017. Original article submitted September 13, 2016.

The increased melting difficulty parameter of carbides ($9.96 \cdot 10^{10}$ kJ^2/kg $\cdot$ m^3 for TiC and 2.28×10^{10} kJ^2/kg $\cdot$ m^3 for Cr_3C_2) [17] indicates that their thermal spraying in pure form can produce coatings with high porosity and decreased adhesion and cohesion strength and wear resistance. One of the ways to increase these characteristics is to introduce a ductile metallic binder into the coating in an amount of 10–25% [16, 18].

The simplest and most common way of producing carbide cermet coatings is to use a carbide–metal mechanical mixture as the starting material. In this case, however, different thermal properties of particulate material such as density, heat capacity, thermal conductivity, and melting point cause separation of the components, starting from their transport by piping and ending with the feeder. Moreover, particles of the mechanical mixture have different paths over the plasma jet, which leads to different conditions of heating and interaction of the particular material and environment, resulting in nonhomogeneous distribution of components in the coating.

In this connection, it is needed to develop coatings of complex composition from composite powder materials, particularly clad powders; i.e., those in which particles of the starting material are uniformly covered with a cladding layer of the other component. The advantage of using a clad powder (provided that the work of adhesion exceeds the surface tension of the liquid cladding layer) is the formation of a continuous melt shell that isolates the carbide material from contact with the environment and thereby reduces carbon losses because of burnout. In addition, under these conditions, the contact surface of two materials is dispersed, promoting uniform composition of the coating and formation of intermetallic compounds [19].

To evaluate the nature of interaction in the Ni–(Ti, Cr)C system, wetting of compact nickel and hot-pressed titanium–chromium carbide samples was studied with the sessile drop method in 1.33 MPa vacuum at 1400–1500°C. Molten nickel is known to wet titanium–chromium carbide so that the contact angle changes from 44 to 9° within 10 sec and then, with increasing contact time, remains virtually the same. The work of adhesion evaluated in these measurements was 3400 mJ/m^2, which is almost twice as high as the surface tension of liquid nickel [20] and is indicative of chemical interaction in the contact zone.

Furthermore, the use of nickel, having relatively higher specific weight, as a cladding layer on (Ti, Cr)C particles increases the average density of a composite powder particle, reduces its velocity in the plasma jet, and facilitates the heating conditions.

The experiments on application of cermet coatings containing double titanium–chromium carbide (Ti, Cr)C involved nickel-clad [12, 18] or nickel–molybdenum-clad [21] composite powders (Ti, Cr)C. The coatings were produced by plasma spraying using an argon–hydrogen mixture as the working gas [12, 18, 20, 21] and by subsonic and supersonic air plasma spraying (APS) [20]. The plasma sprayed coatings produced with an Ar/H_2 plasma jet and 30–35 kW plasma gun power [21] consist of a carbide phase with microhardness HV = 25–30 GPa, a metallic phase with HV = 1.8 GPa, and a phase possessing HV = 15–16 GPa and apparently resulting from interaction of (Ti, Cr)C with the metal of the shell covering Ni particles [15, 21].

Analysis of structural and phase transformations in pure and clad (Ti, Cr)C powders that occur in the APS process shows that supersonic spraying decreases the oxidation of sprayed material and ensures stability of the cladding shell on the carbide core [15]. In this connection, high-velocity spray methods [22] seem to be more preferable as they allow the sprayed material to be accelerated to 300–600 m/sec to provide a spraying efficiency of 40 kg/h and high utilization factor: 50–75% for oxides, carbides, and other refractory compounds and 70–85% for metals and their alloys.

Study of the heat resistance of plasma sprayed coatings from Ni–(Ti, Cr)C composite powder containing 30–35 wt.% Ni shows that they possess quite high oxidation resistance in air at 800°C [12, 16].

The objective of this paper is to determine how plasma spraying parameters influence the structure and properties of coatings from the (Ti, Cr)C–32 wt.% Ni clad composite powder in APS conditions.

MATERIALS AND EQUIPMENT

The starting material to be sprayed was double titanium–chromium carbide (Ti, Cr)C–32 wt.% Ni clad powder with 5–40 μm particles. The titanium–chromium powder was produced by self-propagating high-temperature synthesis (SHS) from a mixture of titanium, chromium, and ash in the ratio TiC : Cr_3C_2 = 7 : 3 [18, 21].

The SHS (Ti, Cr)C powder was clad using electrolytic deposition of a 1–1.5 μm nickel layer on carbide particles. The characteristics of (Ti, Cr)C and Ni are provided below:

Composition, wt.%:
- Double titanium–chromium carbide . . . . . 70 TiC/30 Cr_3C_2
- Nickel. 100

Melting point, °C:
- Double titanium–chromium carbide . . . . . ~2750
- Nickel. 1453

Density, g/cm^3:
- Double titanium–chromium carbide 5.35
- Nickel. 8.9

The coatings were applied using a Kiev-S supersonic air plasma spraying unit developed jointly with the Gas Institute and Paton Electric Welding Institute [23]. Air was used as the plasma gas.

EXPERIMENTAL PROCEDURE

The experimental spraying procedure was developed using blocks (half-replicas) of fractional factorial 2^{3-1} design for different anode nozzle diameters, d_A = 10 and 11 mm (Table 1), with partition of the complete factorial design into blocks [24]. The spraying processes with anode diameters 10 and 11 mm fundamentally differ in the nature of plasma jet. In one case (d_A = 10 mm), the jet is supersonic in all spraying modes. In the other case (d_A = 11 mm), the jet can be considered subsonic, depending on the electric power and plasma gas flow, since it can fall in both subcritical and critical flow ranges.

Plasma gun power W, kW (X_1), plasma gas (air) flow G, m^3/h (X_2), and spraying distance L, mm (X_3) (Table 2) were selected as variable parameters. Flow rate of the sprayed material remained unchanged in all experiments (6 kg/h).

The experimental design developed in compliance with the fractional factorial design is presented in Table 3.

Since one of the main tasks in the plasma spraying of coatings containing carbides is to ensure their wear resistance, we used the following characteristics as response functions in the experimental design:

- HV^{av}—the average microhardness of the coating characterizing its structure and potential wear resistance indicator, GPa;

TABLE 1. Fractional Factorial 2^{3-1} Design

Experiment No.	X_1	X_2	X_3
1	–	–	+
2	–	+	–
3	+	–	–
4	+	+	+
5	–	–	–
6	–	+	+
7	+	–	+
8	+	+	–

TABLE 2. Variation Intervals and Values of APS Coating Parameters

Variation levels	W, kW	L, mm	G, m^3/h
Upper +	100	220	36
Lower –	80	160	26
Basic 0	90	190	31
Variation interval	10	30	5

- $\Delta X/HV^{av}$—the ratio of the confidence interval of microhardness distribution $\Delta X = \frac{1}{n}\sum_{i=1}^{n}\left(HV^{av} - HV^{i}\right)$ to the average microhardness of the coating characterizing the homogeneity of its structure (here HV^{i} is microhardness in each measurement; $n = 35$).

To analyze the relation of the results obtained with the spray process conditions, we used the following parameters:

- $K_T = W/G$, kW · h/m^3—heat content of the plasma jet (heat received by the plasma jet passing in the arc discharge);
- $K_\tau = 2.82 \cdot L \cdot d_A^2/G$, sec—time during which powder particles move in the jet until they hit the substrate;
- $V = G \cdot 4/\pi d_A^2$, m/sec—plasma jet flow rate.

The steel samples were preliminary subjected to abrasive jet treatment with corundum powder. The transport gas flow rate was selected so that the flight path of the (Ti, Cr)C–32 wt.% Ni powder particles was located in the axial zone of the plasma jet.

TABLE 3. Experimental Design for APS of (Ti, Cr)C–32% wt. Ni Powder

Experiment (mode) No.	W, kW	L, mm	G, m^3/h
Anode nozzle diameter 11 mm			
1	80	160	36
2	80	220	26
3	100	160	26
4	100	220	36
Anode nozzle diameter 10 mm			
5	80	160	26
6	80	220	36
7	100	160	36
8	100	220	26

TABLE 4. Characteristics and Properties of the APS (Ti, Cr)C–32 wt.% Ni Coatings Produced in Compliance with the Experimental Design (Table 3)

Experiment (mode) No.	Microhardness $HV_{0.05}$, GPa				Phase constituents*	Porosity, vol.%	Thickness, μm	K_T, kW · h/m^3	K_τ, 10^{-3} sec	V, m/sec
	HV^{av}	HV^{max}	$\Delta X/HV^{av}$	$HV^{m.p}$						
1	13.13	16.52	0.125	15	CrNiTi, (Ti, Cr)C, TiC_{1-x}, Ni, $NiTiO_3$	≤3	200	2.22	1.52	105
2	12.71	16.52	0.107	13	Ni, (Ti, Cr)C, TiC_{1-x}, CrNiTi, $NiTiO_3$	≤2	250	3.08	2.89	76
3	13.87	17.25	0.113	15	(Ti, Cr)C, TiC_{1-x}, CrNiTi	≤2	200	3.85	2.10	76
4	12.15	16.52	0.134	12	Cr, Ni, (Ti, Cr)C, TiC_{1-x}, Cr_2O_3, $NiTiO_3$, CrN, TiN, Cr_2Ti	≤3	150	2.78	2.09	105
5	13.7	21.61	0.2	15	CrNiTi, (Ti, Cr)C, TiC_{1-x}, Ni, $NiTiO_3$, Cr	1–2	325	3.07	1.74	92
6	12.73	17.98	0.17	13	Ni, CrNiTi, TiC_{1-x}, (Ti, Cr)C, $NiTiO_3$, Cr	1–2	250	2.22	1.72	127
7	14.58	21.62	0.155	13; 17	(Ti, Cr)C, TiC_{1-x}, CrNiTi	≤3	200	2.78	1.25	127
8	13.54	19.69	0.137	13	Cr, Ni, (Ti, Cr)C, TiC_{1-x}, Cr_2Ti, $NiTiO_3$, Cr_2O_3, CrN	≤3	325	3.85	2.39	92

* The phases are placed according to lower intensities of reflections, i.e., their contents.

The coating structure was examined with metallography (Neophot-32 microscope) and X-ray diffraction (DRON-3M, Cu-K_α radiation with a Ni filter), and properties with a PMT-3 microhardness meter. The coating porosity was determined in the dark field of the metallographic section.

EXPERIMENTAL RESULTS AND DISCUSSION

Table 4 summarizes results from examining the structure and properties of the coatings produced in accordance with the experimental design pursuant to Table 3. The microstructure of the coatings sprayed in the modes in compliance with the experimental design is shown in Fig. 1, and variation curves for microhardness of the coatings that were used to determine the most probable microhardness values, $HV^{m.p}$, are provided in Fig. 2.

Metallographic analysis of the sprayed coatings revealed no fundamental differences in their structure depending on spray mode. The microstructure of the coatings (Fig. 1) indicates that they have high density (porosity to 3%), contain no inclusions of unmolten particles, and are highly homogeneous. The coatings properly adhere to the substrate (no delamination is observed). However, the coatings differ in the average microhardness and nature of the variation curves (Fig. 2).

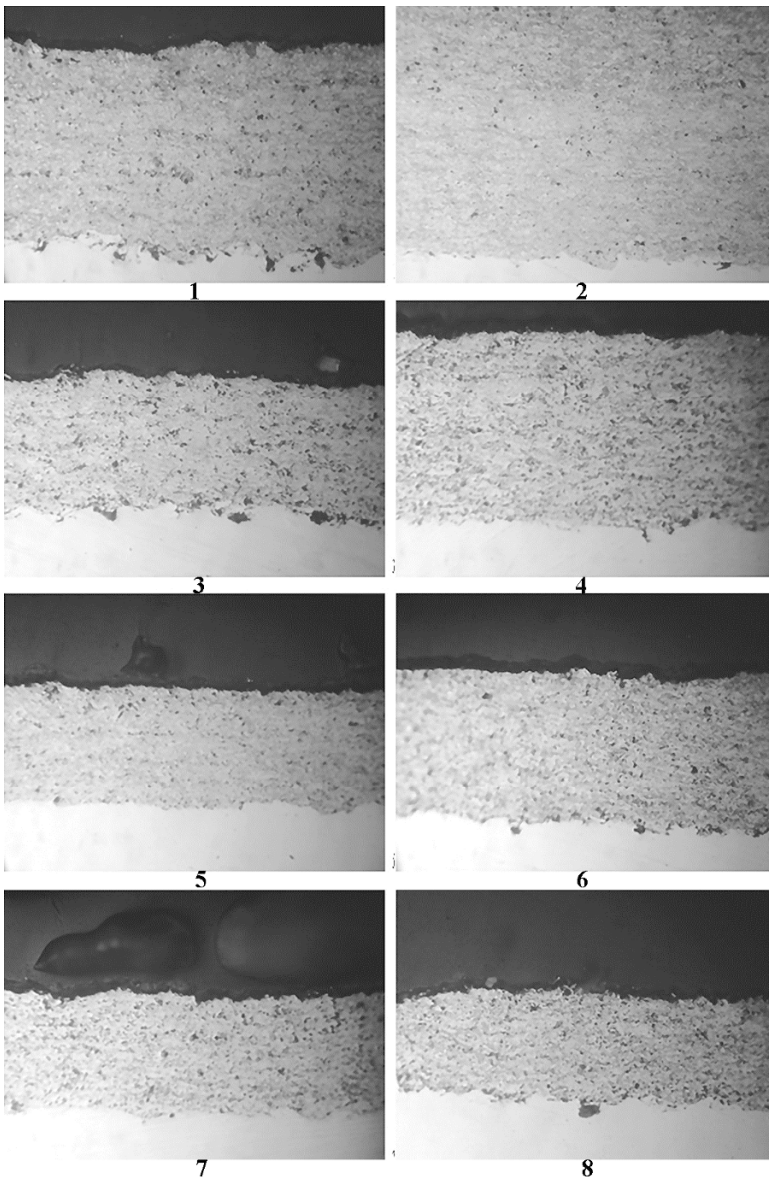

Fig. 1. Microstructure of the (Ti, Cr)C–32 wt.% Ni coatings sprayed in APS modes 1–8 (Table 3); ×200

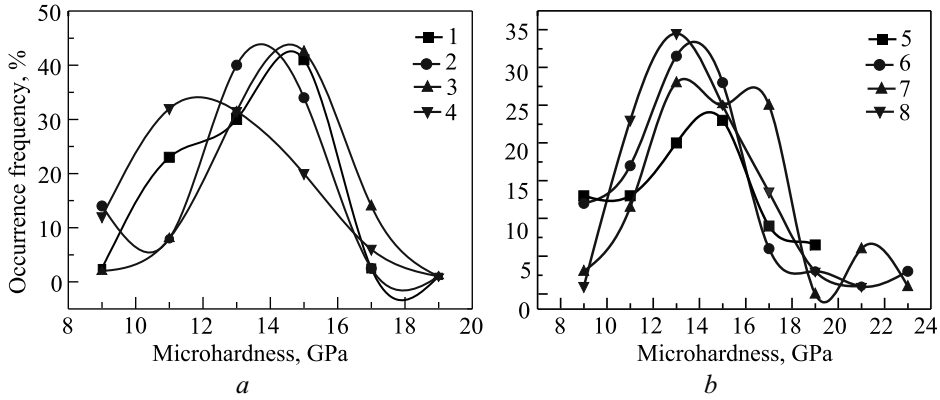

Fig. 2. Variation curves for microhardness of the (Ti, Cr)C–32 wt.% Ni coatings sprayed in APS modes 1–8 (Table 3): anode nozzle diameter 11 (*a*) and 10 (*b*) mm

The most prominent two-phase structure consisting of (Ti, Cr)C and TiC_{1-x} carbides in the metallic CrNiTi matrix was found in the coatings sprayed in experiments 3 and 7. Figure 3 shows X-ray diffraction patterns with indication of phase constituents of the coatings sprayed in the modes in compliance with the experimental design (Table 3) and coatings from the starting (Ti, Cr)C–32 wt.% Ni powder.

Summary data on characteristics of the (Ti, Cr)C–32 wt.% Ni coatings sprayed in compliance with the experimental design (Table 3) are provided in Table 4.

The production of APS coatings from the (Ti, Cr)C–32 wt.% Ni clad powder is associated with the processes that occur within the particle when heated and moving in the plasma jet. There is a number of distinctions compared to spaying of (Ti, Cr)C–25 wt.% NiCr mechanical mixtures [25], in which high heat content K_T of the plasma jet and longer heating K_τ of particles are necessary conditions because lower-melting NiCr melts first, and contribution of components to the (Ti, Cr)C coating depends on heat-exchange processes. Spraying of the (Ti, Cr)C–32 wt.% Ni clad powder with higher average density (because of a Ni layer) promotes more favorable conditions for producing the coating since, in this case, there are no difficulties that occur as the particle has no time to heat up in the plasma jet because it has low density and high melting point.

Another advantage of the clad powder is that the nickel melt forms a shell on carbide particles to isolate the core from contact with the environment and, thus, minimize losses of carbon when the particles move in the jet oxygen-containing zones. The coatings from (Ti, Cr)C–32 wt.% Ni clad powder possess higher microhardness (12.15–14.58 GPa) than those produced from the 75 wt.% (Ti, Cr)C + 25 wt.% NiCr (5.3–12.6 GPa) mechanical mixture [25]. In addition, development of the carbide/matrix contact surface promotes the formation of homogenous composite coatings and intermetallic compounds. Active interaction between the Ni shell of the clad powder and (Ti, Cr)C particles leads to the CrNiTi phase, as well as intermetallic Cr_2Ti and chromium, in the coatings.

The qualitative composition of the samples in experiments 1 and 5, 2 and 6, 3 and 7, and 4 and 8 differ in the ratio of metallic, carbide, and oxide phases. The most active interaction between components of the composite powder is observed in experiments 4 ($K_T = 2.78$ kW · h/m^3, $K_\tau = 2.09 \cdot 10^{-3}$ sec) and 8 ($K_T = 3.85$ kW · h/m^3, $K_\tau = 2.39 \cdot 10^{-3}$ sec), which leads to the Cr, Cr_2O_3, and Cr_2Ti phases and chromium nitride traces in the coatings. The most homogeneous coatings were produced in modes 3 ($K_T = 3.85$ kW · h/m^3, $K_\tau = 2.10 \cdot 10^{-3}$ sec) and 7 ($K_T = 2.78$ kW · h/m^3, $K_\tau = 1.25 \cdot 10^{-3}$ sec), whose phase composition is presented by (Ti, Cr)C and TiC_{1-x} carbides and CrNiTi matrix.

Therefore, analysis of the coating phase composition (Fig. 3 and Table 4) indicates that a series of processes occur when the (Ti, Cr)C–32 wt.% Ni composite powder is being sprayed and heated and moves in the plasma jet. These processes results in the following changes in the phase composition of the material sprayed:

- nickel shell of the (Ti, Cr)C–32 wt.% Ni composite powder interacts with the carbide core to form CrNiTi and Cr_2Ti;

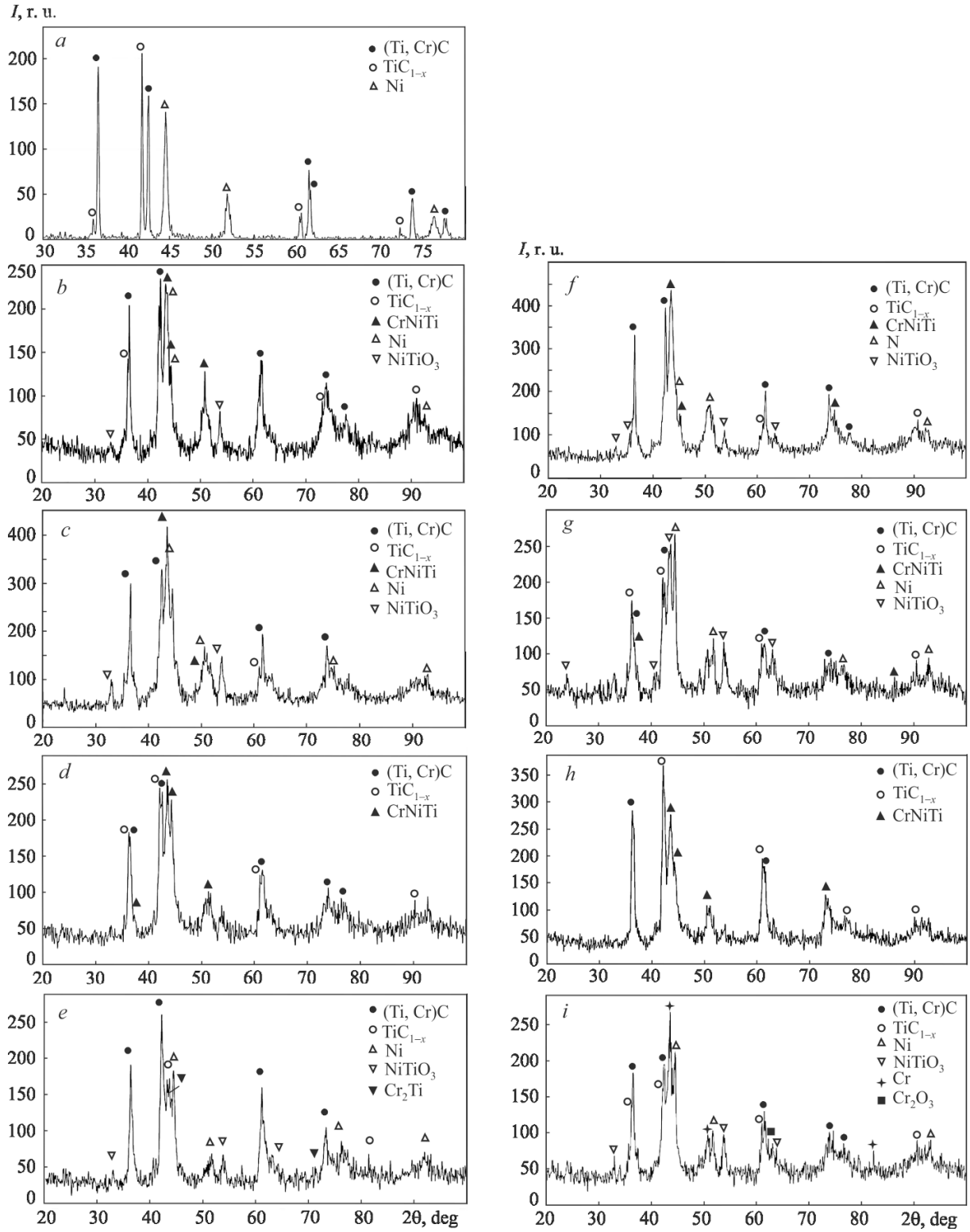

Fig. 3. X-ray diffraction patterns for the starting powder (*a*) and (Ti, Cr)C–32 wt.% Ni coatings spayed in APS modes (Table 3): 1 (*b*); 2 (*c*); 3 (*d*); 4 (*e*); 5 (*f*) 6 (*g*); 7 (*h*), and 8 (*i*)

- carbide is intensively heated as a result of thermal impact of the plasma jet on (Ti, Cr)C–32 wt.% Ni particles, should they stay for a long time within the plasma jet, which leads to loss of carbon and partial decomposition of (Ti, Cr)C to TiC_{1-x} and Cr;

- because of inadequate heating (when the powder particle moves along the jet periphery where gas temperature is lower than the melting point of (Ti, Cr)C–32 wt.% Ni), particles remain unmolten or partially molten and the Ni shell, without reacting with the (Ti, Cr)C carbide core, is present as pure nickel in the coating; it may be present in the coating because of thermal and dynamic impact of the plasma jet on sprayed particles, which may cause the lower-melting metallic nickel shell to break away from the carbide core;
- oxygen and nitrogen of the plasma jet and the environment interact with components of the sprayed particle to form mainly $NiTiO_3$ and an insignificant amount of Cr_2O_3, CrN, and TiN.

To determine the effect of individual factors of the spray process on coating characteristics (average microhardness HV^{av} and ratio of the confidence interval of microhardness distribution to the average microhardness of the coating, $\Delta X/HV^{av}$, which reflects the homogeneity of its structure), the following regression equations were derived from the data obtained in accordance with the experimental design pursuant to Tables 3 and 4:

$$HV^{av} = 17.96 + 0.0045W - 0.0178L - 0.065G,$$

$$\Delta X/HV^{av} = 0.0208 + 0.000375W + 0.000025L + 0.00195G$$

for anode diameter 11 mm;

$$HV^{av} = 12.91 + 0.04255W - 0.01675L + 0.0035G,$$

$$\Delta X/HV^{av} = 0.4356 - 0.00195W - 0.0004L - 0.0006G$$

for anode diameter 10 mm.

Comparison of the experimental results and calculated data (Table 5) shows that the regression equations with high accuracy (more than 0.99) describe the effect exerted by the spray process factors on coating characteristics, which is evidenced by Student's criterion: it is close to 0 in case of HV^{av} and is equal to 0 in case of $\Delta X/HV^{av}$.

The regression equations were used to plot trend lines that reflect the degree with which individual factors influence the coating characteristics (Fig. 4).

The nature and intensity with which various factors influence coating characteristics (in selected experimental domain) are compared using the trends (Fig. 4), and comparison results are provided in Table 6. The greatest effect on microhardness HV^{av} and parameter $\Delta X/HV^{av}$, characterizing the reproducibility of coating properties, is exerted by the plasma gas flow and plasma gun power. The spraying distance insignificantly influences the properties, and microhardness somewhat decreases with longer spraying distance. This may be because the (Ti, Cr)C core surface is actively wetted by the lower-melting clad material (nickel) in the spraying process and, thus, the particle flight distance range in which the coating may form expands compared to unclad powder.

Table 6 shows that the effect of plasma gun power on the trends (Fig. 4) in use of anode nozzle diameter d_A = 10 and 11 mm is unidirectional—only does intensity of this effect change. With higher plasma gun power, heat content of the plasma jet increases and heating of particles intensifies, improving HV^{av} and $\Delta X/HV^{av}$. In the case of

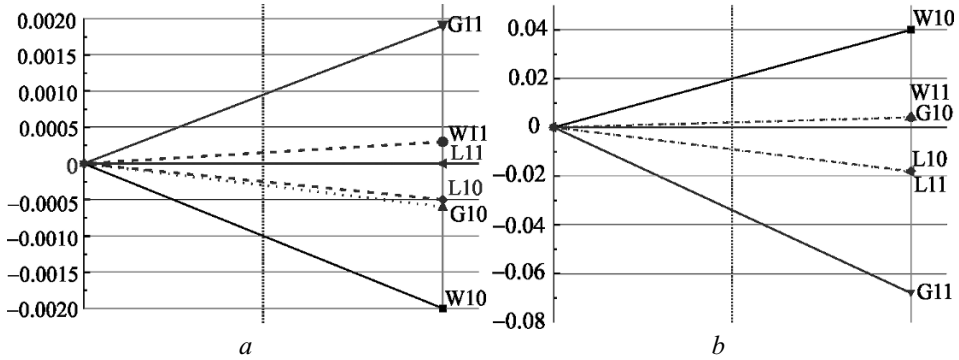

Fig. 4. Effect of APS factors on characteristics of the (Ti, Cr)C–Ni coatings: *a*) HV^{av}; *b*) $\Delta X/HV^{av}$

TABLE 5. Comparison of Experimental and Calculated Data Obtained from Regression Equations

Sample No.	HV^{av}_{exp}, GPa	HV^{av}_{calc}, GPa	ΔHV^{av}, GPa
Anode nozzle diameter 11 mm			
1	13.13	13.135	–0.005
2	12.71	12.714	–0.004
3	13.87	13.87	0
4	12.15	12.154	–0.004
Anode nozzle diameter 10 mm			
5	13.7	13.701	–0.001
6	12.73	12.731	–0.001
7	14.58	14.581	–0.001
8	13.54	13.541	–0.001
Sample No.	$\Delta X / HV^{av}_{exp}$, GPa	$\Delta X / HV^{av}_{calc}$, GPa	$\Delta X/HV^{av}$, GPa
Anode nozzle diameter 11 mm			
1	0.125	0.125	0
2	0.107	0.107	0
3	0.113	0.113	0
4	0.134	0.134	0
Anode nozzle diameter 10 mm			
5	0.2	0.2	0
6	0.17	0.17	0
7	0.155	0.155	0
8	0.137	0.137	0

TABLE 6. Effect of APS Factors on the Properties of the (Ti, Cr)C–32 wt.% Ni Coatings*

Properties	*W*		*G*		*L*	
	d_A = 10 mm	d_A = 11 mm	d_A = 10 mm	d_A = 11 mm	d_A = 10 mm	d_A = 11 mm
HV^{av}	↑↑	↑	↑	↓↓	↓	↓
$\Delta X/HV^{av}$	↑↑	↓	↑	↓↓	~	~

*↑↑, ↓↓—strong; ↑, ↓—moderate; ~—weak.

subsonic plasma jet (with d_A = 11 mm), the effect of factor *W* is much weaker, though the tendency to improving the indicators with higher plasma gun power remains in place.

Higher plasma gas flow in use of anode nozzle diameter 10 mm leads to a slight increase in microhardness HV^{av} and coating homogeneity indicator $\Delta X/HV^{av}$. Contrastingly, in use of anode nozzle diameter 11 mm, this sharply decreases the characteristics in question.

This strong effect of the plasma gas on the coating characteristics in use of anode nozzle diameter 11 mm is probably due to the instability of plasma jet, changing from subcritical to critical with higher plasma gas flow at the maximum plasma gun power. This influences the development of heat-exchange and dynamic gas processes in coating spraying.

CONCLUSIONS

A series of experiments on air plasma spraying of the (Ti, Cr)C–32 wt.% Ni clad powder using the mathematical planning method allowed us to analyze how the process parameters (plasma gun power, plasma gas flow, spraying distance, plasma jet nature) influence the structure and properties of the resultant coatings (microstructure, phase composition, microhardness, porosity). Coatings with 1–3 vol.% porosity that strongly adhere to the substrate form in all cases.

The maximum microhardness (HV^{av} = 13.87 GPa, HV^{max} = 17.25 GPa) and (HV^{av} = 14.58 GPa, HV^{max} = = 21.62 GPa) is reached in experiments 3 and 7, which are characterized by an optimum combination of thermal and kinetic energy of the particles depending on the heat content of plasma jet, $K_T = W/G$, kW · h/m^3, and plasma jet flow rate, $V = G \cdot 4/\pi d_A^2$, m/sec. The phase composition is presented by (Ti, Cr)C, TiC_{1-x} and CrNiTi without any oxides. The CrNiTi phase results from interaction of the Ni shell and (Ti, Cr)C particles and serves as a matrix for forming the cermet coating.

The hardness of APS coatings from (Ti, Cr)C–32 wt.% Ni clad powder (12.15–14.58 GPa) is higher than that in use of the 75 wt.% (Ti, Cr)C + 25 wt.% NiCr mechanical mixture (5.3–12.6 GPa) since the carbide oxidation and carbon loss processes are limited.

The differences in regression equations and trends for the APS coatings from the (Ti, Cr)C–32 wt.% Ni powder at d_A = 10 and 11 mm are due to the heating conditions and phase phenomena in the spraying process, which are associated with change in the nature of plasma jet. In one case (d_A = 10 mm), the plasma jet is supersonic in all spraying modes. In the other case (d_A = 11 mm), the plasma jet may be considered subsonic, depending on electric power and plasma gas flow, and may fall in both subcritical and critical flow ranges.

REFERENCES

1. D. Toma, W. Brandtt, and G. Marginean, "Wear and corrosion of thermally sprayed cermet coatings," *Surf. Coat. Technol.*, **138**, 149–158 (2001).
2. P. Sahoo and R. Raghuraman, "High temperature chromium carbides reinforced metal matrix composite coatings for turbomachinery application," in: *Proc. Thermal Spray Conf. (TS'93)*, DVS-Berichte, Aachen, Germany (1993), pp. 296–300.
3. J. Takeuchi and A. Nakahira, "Cr_3C_2–NiCr cermet coatings using some HVOF, APS and UPS process," *Proc. Thermal Spray Conf. (TS'93)*, DVS-Berichte, Aachen, Germany (1993), pp. 11–14.
4. N. Espallargas, J. Berget, J. M. Guilemany, et al., "Cr_3C_2–NiCr and WC–Ni spray coatings as alternatives to hard chromium for erosion–corrosion resistance," *Surf. Coat. Technol.*, **202**, 1405–1417 (2008).
5. J. Beczkowiak, J. Fisher, and Y. Schwier, "Cermet materials for HVOF processes," in: *Proc. Thermal Spray Conf. (TS'93)*, DVS-Berichte, Aachen, Germany (1993), pp. 32–36.
6. H. Keller, E. Pross, and G. Schwier, "Influence of the powder type on the structure and the properties of chromium carbide–nickel chromium," in: H. C. Starck (ed.), *Specialist for Specialties* (2000), L11, p. 8.
7. *Powder Solutions Catalog*, Praxair Surface Technologies (2000), p. 17.
8. *Thermal Spray Materials Guide*, Sulzer Metco, USA (2011), p. 52.
9. E. Lugscheider, P. Remer, C. Herbst, et al., "NiCr–Cr_3C_2 and NiCr–TiC high wear resistant coatings for protective applications in steam turbines," in: *Proc. Thermal Spray Conf. (TS'95)*, DVS-Berichte, Aachen, Germany (1995), pp. 235–240.
10. V. N. Shukla, V. K. Tewari, and R. Jayagantthan, "Comparison of tribological behavior of Cr_3C_2/NiCr coatings deposited by different thermal spray techniques," in: *Proc. ITSC'2011*, DVS-Berichte, Gamburg, Germany (2011).
11. R. Kieffer and F. Benezovsky, *Hardmetals* [in German], Springer-Verlag, Vienna (1963).
12. I. N. Gorbatov, V. M. Shkiro, A. E. Terentiev, et al., "Studying the properties of thermal spray coatings from nickel–titanium and chromium carbide powders," *Fiz. Khim. Obrab. Mater.*, No. 4, 102–106 (1991).

13. R. F. Voitovich and E. A. Pugach, “High-temperature oxidation characteristics of the carbides of the group VI transition metals,” *Powder Metall. Met. Ceram.*, **12**, No. 4, 314–318 (1973).
14. R. F. Voitovich and E. A. Pugach, *Oxidation of Refractory Compounds* [in Russian], Naukova Dumka, Kyiv (1968), p. 84.
15. S. S. Kiparisov, Yu. V. Levinskii, and A. P. Petrov, *Titanium Carbide: Production, Properties, Application* [in Russian], Metallurgiya, Moscow (1987), p. 218.
16. V. B. Raitses, V. M. Litvin, V. P. Rutberg, et al., “Wear-resistant plasma coatings based on a double carbide of titanium and chromium,” *Powder Metall. Met. Ceram.*, **25**, No. 10, 827–828 (1986).
17. Yu. S. Borisov, *Powders for Thermal Spraying of Coatings* [in Russian], Znanie, Kyiv (1984), p. 15.
18. I. N. Gorbatov, N. S. Il’chenko, A. E. Terentiev, et al., “Effect from cladding of double titanium–chromium carbide on properties of plasma spayed coatings,” *Fiz. Khim. Obrab. Mater.*, No. 3, 81–85 (1991).
19. A. Ya. Kulik, Yu. S. Borisov, A. S. Mnukhin, and M. D. Nikitin, *Thermal Spraying of Composite Coatings* [in Russian], Mashinostroenie, Leningrad (1985), p. 199.
20. I. N. Gorbatov, A. D. Panasyuk, L. K. Shvedova, et al., “Thermal spray coatings from titanium–chromium carbide composite powders,” *Prot. Coat. Met.*, Issue 25, 22–25 (1991).
21. A. L. Borisova and A. I. Chernets, “Phase and structural transformations in powders of pure and clad double titanium–chromium carbide in a plasma jet,” *Probl. SEM,* No. 3, 63–72 (1993).
22. Yu. Borisov, M. Kolomytsev, and A. Borisova, “Tungsten carbide–cobalt coatings produced by supersonic air–gas plasma spraying,” in: *Proc. 14th Int. Plansee Seminar*, Reutte, Austria (1997), Vol. 3, pp. 330–341.
23. Yu. S. Borisov and S. V. Petrov, “Use of supersonic jets in thermal spraying process,” *Avtomat. Svarka*, No. 1, 24–34 (1993).
24. A. M. Tamrazov, *Planning and Analysis of Regression Experiments in Engineering Studies* [in Russian], Naukova Dumka, Kyiv (1987), p. 176.
25. Yu. S. Borisov, A. L. Borisova, M. V. Kolomytsev, and O. P. Masyuchok, “Supersonic air fuel thermal spraying of cermet coatings in the titanium–chromium carbide–nichrome system,” *Avtomat. Svarka*, No. 2, 21–27 (2015).